

Hall C - Hypernuclei

G.M. Urciuoli

Three are the goals of the present hypernuclear program at JLab:

- Neutron star structure investigation (solution of the “hyperon puzzle”)
- Charge symmetry breaking study in hyperon – nucleon interaction
- Study of nucleus deformations

In all of them JLab12 members are spokespersons

Despite this program address different topics, the experimental method to achieve all the aforementioned goals is the same: hypernuclear spectroscopy that has to be performed with the best achievable energy resolution and the best achievable binding energy measurement precision.

Because of that, all the experiments that are being proposed to achieve the Jlab hypernuclear program goals will employ the same identical experimental apparatus (but the target).

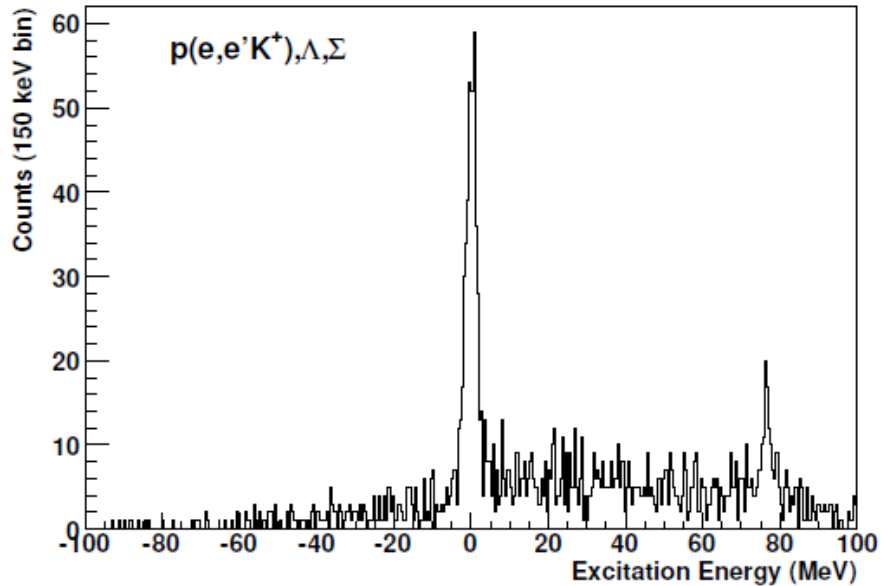
Hypernuclear spectroscopy:

All the present Jlab hypernuclear program proposed experiments will determine with very high precision binding energies of hypernuclei produced by the reaction:



The highly monochromatic CEBAF electrons will be used as incident beam and scattered electron and produced kaons momenta will be determined with high precision spectrometers.

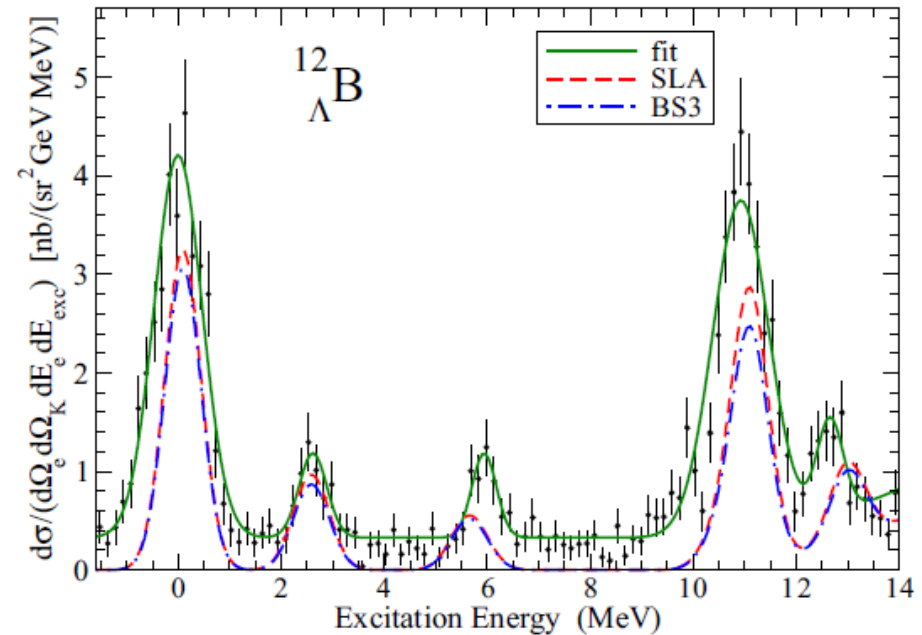
Features of the hypernuclear spectroscopy performed through ${}^A_Z(e, e' K^+) {}^A_{\Lambda}(Z - 1)$ reactions:



Energy calibration

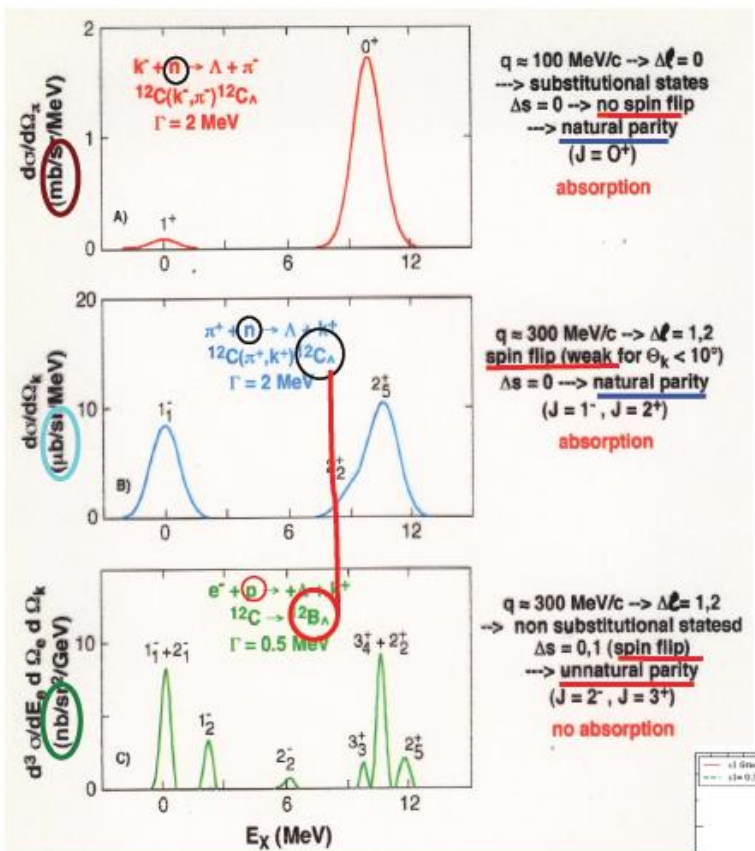
Thanks to the availability of Hydrogen targets and hence to the possibility to determine the excitation energy spectrum of the reaction:

${}^1\text{H}(e, e' K^+)_{\Lambda, \Sigma}$ it is possible to obtain very good **energy calibration** and hence to determine very precisely binding energies



Energy resolution:

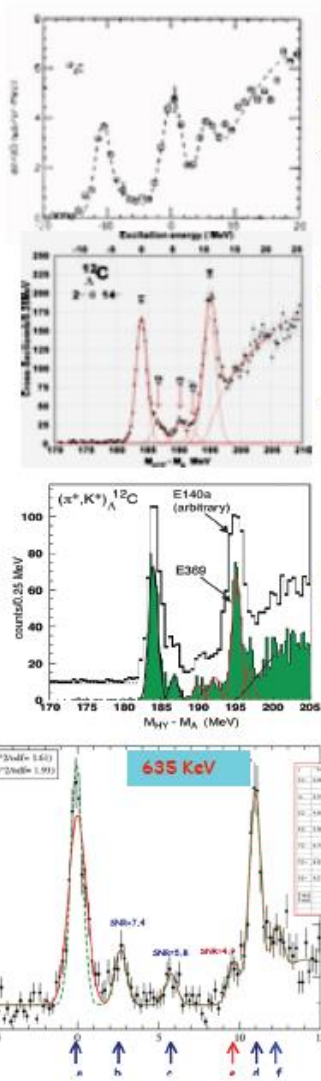
thanks to high resolution spectrometers and the high monochromatic incident electron beam sub-MeV energy resolutions were obtained at Jlab



new aspects of hypernuclear structure

production of mirror hypernuclei

energy resolution $\sim 500 \text{ KeV}$



Improving energy resolution

and

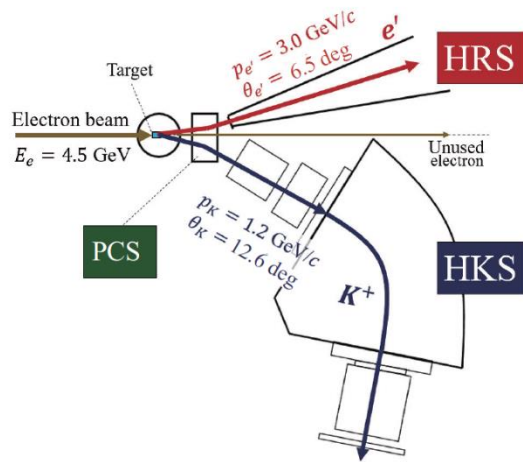
using electromagnetic probe

High resolution, high yield, and systematic study is essential

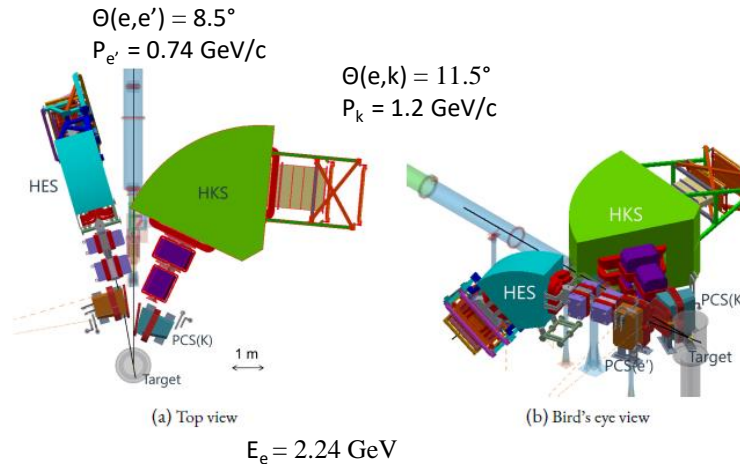
(e,e'K⁺) hypernuclear spectroscopy provides information on the cross section as well as on the binding energy. These information are complementary to the information obtained by decay product studies such as gamma and decay-pion spectroscopies

The experimental apparatus:

Experimental setup and kinematics as originally planned (the experiments were supposed to run in Hall A)



The new Experimental setup and kinematics after moving in Hall C



The Jlab hypernuclear program was initially supposed to run in Hall A. Four experiments were approved to run in this experimental Hall: E12-15-008 (${}^{40}_{\Lambda}K$ and ${}^{48}_{\Lambda}K$ spectroscopy) and E12-20-013 (${}^{208}_{\Lambda}Tl$ spectroscopy) concerning the understanding of neutron star structure, and E12-19-002 (measurements of the binding energy of ${}^3_{\Lambda}H$ and ${}^4_{\Lambda}H$) and C12-20-003 (conditionally approved, investigating the possible existence of a $nn\Lambda$ resonance) to study the CSB. Because of the schedule of the experiment MOLLER that will run in Hall A, to avoid postponing too much the hypernuclear spectroscopy experiments, JLab management prompted the Jlab hypernuclear collaboration to move from Hall A to Hall C. This change has the advantage to improve very much the resolution, but the consequent kinematics change reduces the cross sections and consequently the Signal over Noise ratio and the experimental setup in Hall C forbids the use of gaseous targets. For this reasons, the proposals PR12-24-013 and PR12-24-003, that are the updating of the proposals E12-15-008 and E12-20-013 (neutron star structure studies) in order to adapt them to Hall C apparatus are being submitted to Jlab PAC 52, while the CSB studies were substantially changed with the submission of the new proposal PR12-24-004 (${}^6_{\Lambda}He$, ${}^9_{\Lambda}Li$, and ${}^{11}_{\Lambda}Be$ spectroscopy) and the Run Group Addition E12-20-013A/E12-15-008A (spectroscopy of the hypernuclei and hypernuclear fragments produced in the aforementioned experiments).

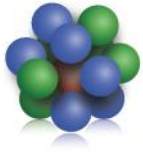
Beam	$\Delta p/p$	$< 1 \times 10^{-4}$ FWHM
	E_e	4.5 GeV
PCS + HRS (e')	D(PCS) + QQDQ	
	$\Delta p/p$	2.6×10^{-4} FWHM
	$p_{e'}$	$3.0 \text{ GeV}/c \pm 4.5\%$
	$\theta_{ee'}$	$6.5 \pm 1.5 \text{ deg}$
	Solid angle $\Omega_{e'}$	2.4 msr
PCS + HKS (K^+)	D(PCS) + QQD	
	$\Delta p/p$	4.2×10^{-4} FWHM
	p_K	$1.2 \text{ GeV}/c \pm 10\%$
	θ_{eK}	$12.6 \pm 4.5 \text{ deg}$
	Solid angle Ω_K	7 msr
	Optical length	12 m
	K^+ survival ratio	26%

Item	Value	
Beam (e)	Energy (/GeV)	2.24
	(Required) energy spread and drift	1×10^{-4} (FWHM)
PCS + HES (e')	Central momentum $p_{e'}^{\text{cent.}}$ [/(GeV/c)]	0.74
	Central angle $\theta_{ee'}^{\text{cent.}}$	8.5°
	Solid angle acceptance $\Omega_{e'}$ (/msr) (at $p_{e'}^{\text{cent.}}$)	3.4
	Momentum resolution $\Delta p_{e'}/p_{e'}$	4.4×10^{-4} (FWHM)
PCS + HKS (K^+)	Central momentum $p_{K^+}^{\text{cent.}}$ [/(GeV/c)]	1.20
	Central angle $\theta_{eK^+}^{\text{cent.}}$	11.5°
	Solid angle acceptance Ω_{K^+} (/msr) (at $p_{K^+}^{\text{cent.}}$)	7.0
	Momentum resolution $\Delta p_{K^+}/p_{K^+}$	2.9×10^{-4} (FWHM)
$p(e, e'K^+)\Lambda$	$\sqrt{s} = W$ (/GeV)	1.912
	Q^2 [/(GeV/c) 2]	0.036
	K^+ scattering angle wrt virtual photon, $\theta_{\gamma-K^+}$	7.35°
	ϵ	0.59
	ϵ_L	0.0096

Neutron star structure

experiments

(hyper)nuclei



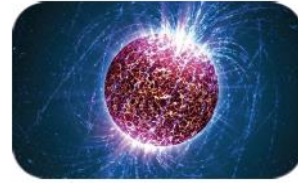
$$R \sim \text{fm} \sim 10^{-15} \text{ m}$$

$$M \sim 10^{-27} \text{ kg}$$

same underlying physics
 \longleftrightarrow
 nuclear force

theory

neutron stars



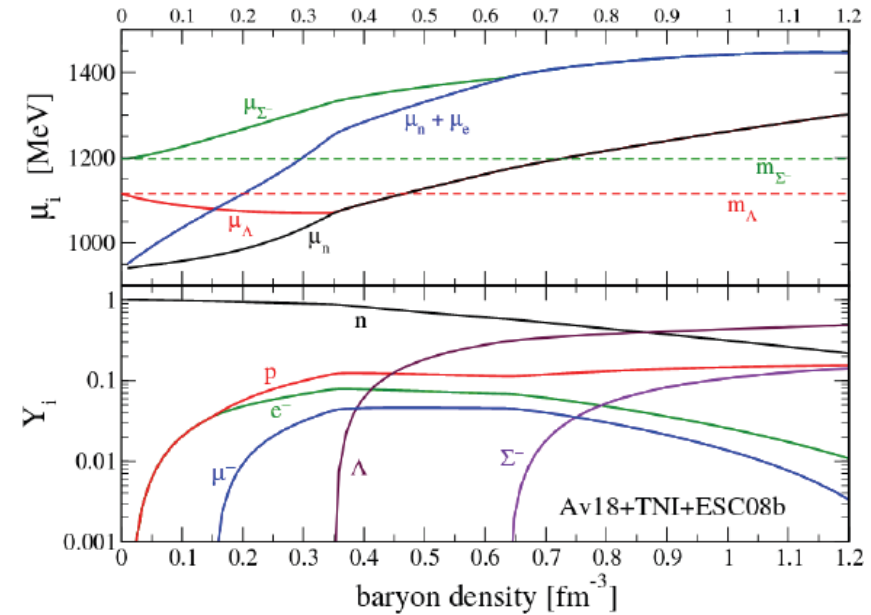
$$R \sim 10 \text{ km} \sim 10^4 \text{ m}$$

$$M \sim 1.4 M_{\odot} \sim 10^{30} \text{ kg}$$

observations

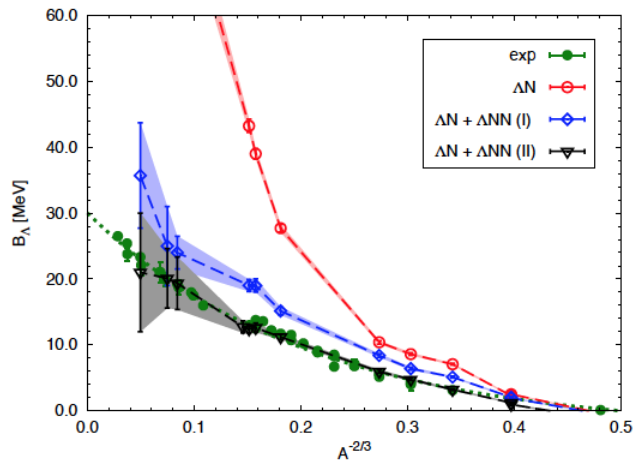
Hyperons are expected to appear in their core at $r \sim (2-3)r_0$ when m_N is large enough to make conversion of N to Y energetically favorable. However, this results in a reduction of the Fermi pressure exerted by the baryons and a softening of the equation of state (EOS). As a consequence, the maximum mass determined by the equilibrium condition between gravitational and nuclear forces is reduced. Most of EOS of matter containing strangeness predict a maximum neutron star mass of about 1.5 solar masses. However, the recent measurements of neutron star masses as big as 2 solar masses require a much stiffer EOS (Hyperon puzzle).

Neutron stars are remnants of the gravitational collapse of massive stars having masses of (1-2 solar masses $\sim 2 \times 10^{33}$ Kg) and are excellent observatories to test fundamental properties of nuclear matter under extreme conditions and offer interesting interplay between nuclear processes and astrophysical observables

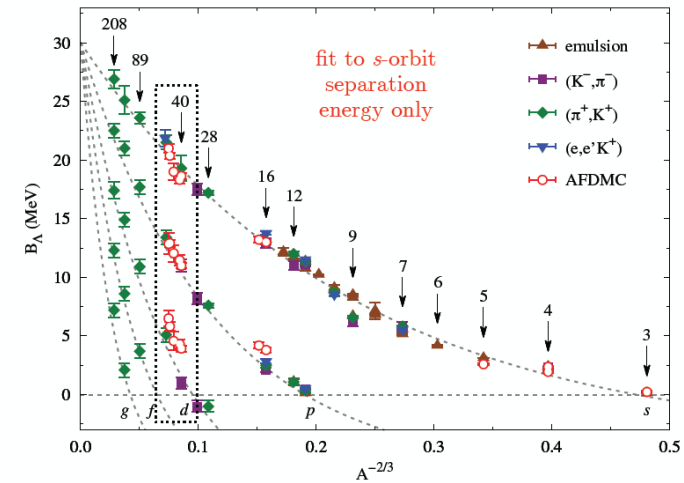


The hypothesis that Neutron Star masses cannot be greater than 1.5 solar masses derived from the assumption that the attractive **interaction between Λ and nucleons**, experimentally confirmed **only at the normal nuclear density (ρ_0)**, holds true also when one deals with higher density nuclear matter. To solve the hyperon puzzle it has been suggested that **three body forces could provide additional repulsion making the EOS stiffer enough**. This hypothesis is justified by the observation that realistic NN interaction models, which describe **all the NN scattering data and light nuclei** (by adding attractive NNN 3BF), **fail to reproduce the nuclear saturation density ρ_0** . This indicates that **a repulsive, short-range 3BF is present in the interaction between nucleons**. It is natural to hence to **postulate a similar repulsive ΛNN (and $\Lambda\Lambda N, \Lambda\Lambda\Lambda$) interaction**. **However, this has to be proved experimentally!**

D. Lonardoni et al.



the effect of including the ΔNN term in the Hamiltonian is very strong. It provides the repulsion necessary to realistically reproduce the limiting value of B_Λ



D. L. and F. Pederiva, arXiv:1711.07521

I. Vidana et al.

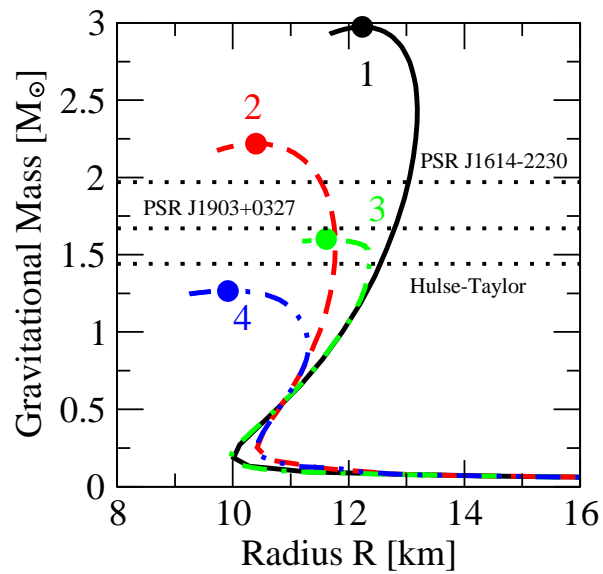
Effect of NNA interaction on hypernuclei

Λ separation energy in $^{41}_\Lambda\text{Ca}$, $^{91}_\Lambda\text{Zr}$ & $^{209}_\Lambda\text{Pb}$

	$^{41}_\Lambda\text{Ca}$	$^{91}_\Lambda\text{Zr}$	$^{209}_\Lambda\text{Pb}$
NSC97a	23.0	31.3	38.8
NSC97a+NNA ₁	14.9	21.1	26.8
NSC97a+NNA ₂	13.3	19.3	24.7
NSC97e	24.2	32.3	39.5
NSC97e+NNA ₁	16.1	22.3	27.9
NSC97e+NNA ₂	14.7	20.7	26.1
Exp.	18.7(1.1)*	23.6(5)	26.9(8)

Only hypernuclei described as a closed shell nuclear core + a Λ sitting in a s.p. state are considered. Comparison with the closest hypernucleus for which exp. data is available

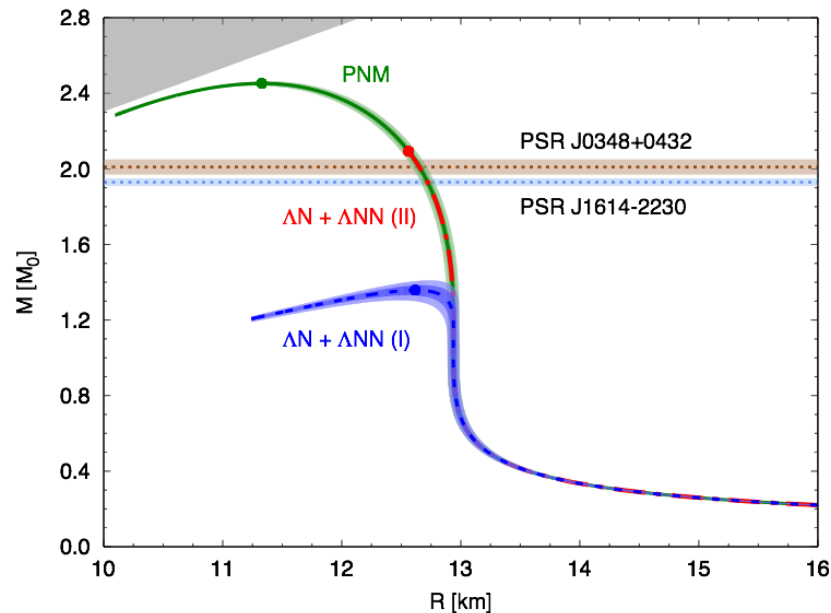
Inclusion of ΔNN improves the agreement with data for $^{91}_\Lambda\text{Zr}$ & $^{209}_\Lambda\text{Pb}$.



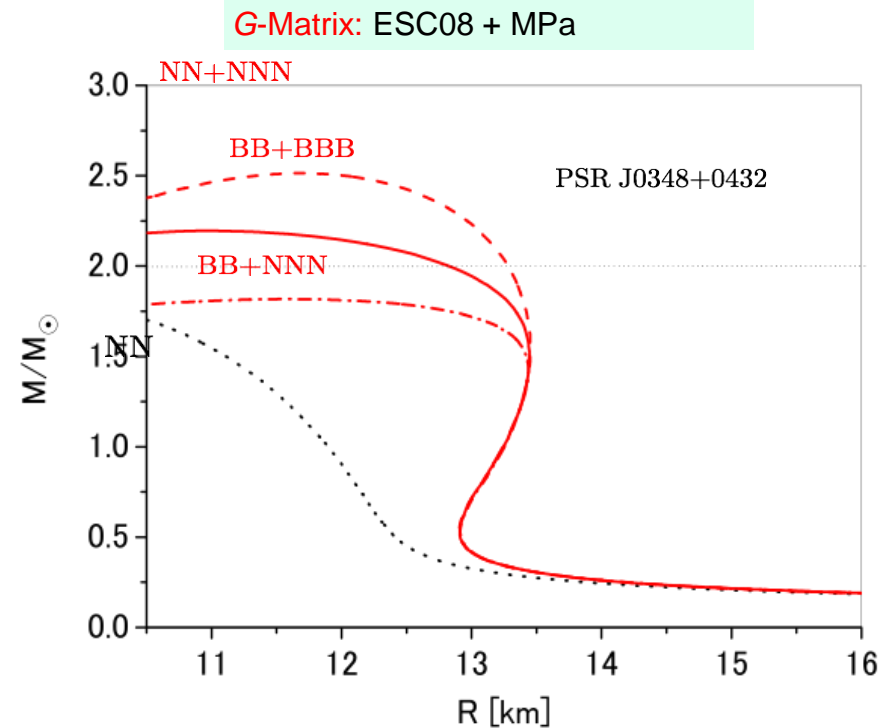
It clearly appears that the inclusion of YNN forces (curve 3) leads to a large increase of the maximum mass, although the resulting value is still below the two solar mass line.

1. Nucleons without 3 body forces
2. Nucleons with 3 body forces
3. Λ and N with 3 body forces (Λ NN)
4. Λ and N without 3 body force

D.Lonardoni *et al.*, Phys. Rev. Lett. 114, 092301 (2015) (AFDMC)



Y. Yamamoto *et al.*, Phys. Rev. C 90, 045805 (2014)



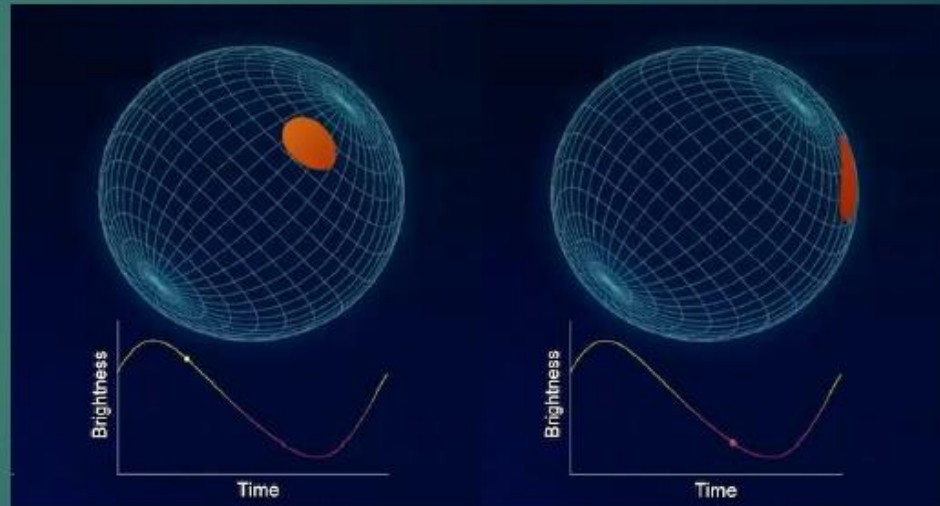
New astronomical observations

New Gravitational Waves from NS mergers and NICER (Neutron star Interior Composition Explorer)



CC4.0 ESO/L. Calçada/M. Kommeser

Gravitation Wave from neutron star mergers
LIGO/Virgo PRL 119, 161101 (2017)

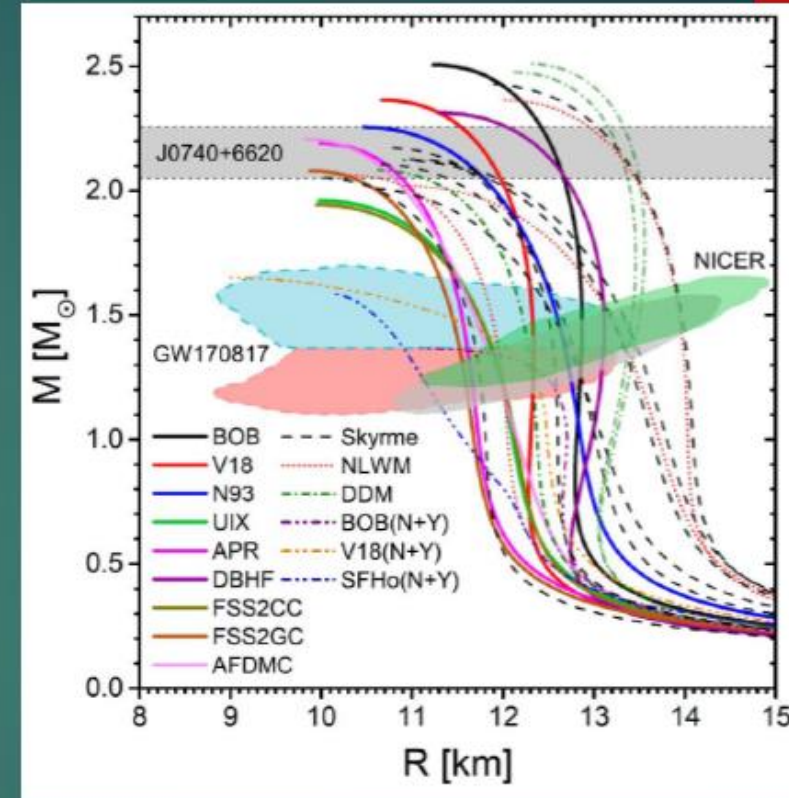
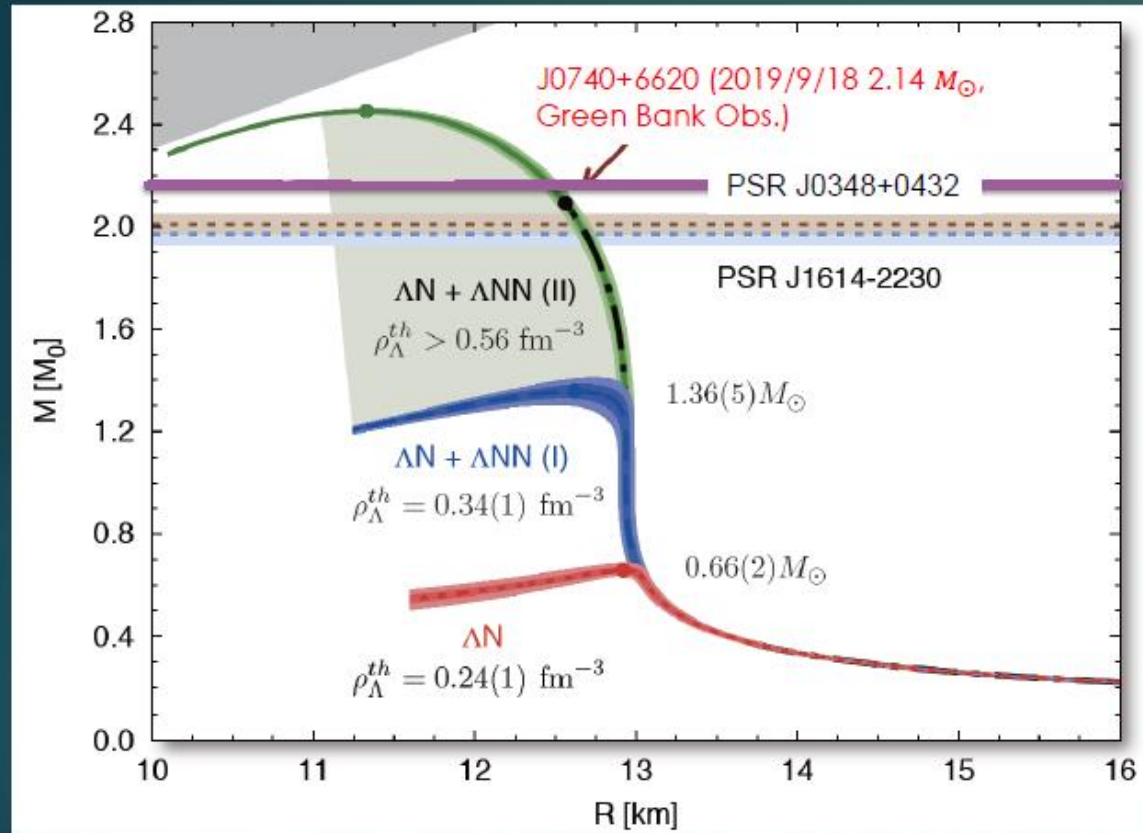


Goddard Space Flight Center

NICER : NS x-ray hot spot measurement
Physics 14, 64 (Apr. 29, 2021)

Macropscopic features of NS : Tidal deformability, Radius and Mass

New constrains from astronomical observations



C.F.Burgio et al. Prog. Part. Nucl. Phys 120 (2021) 103879.

Macroscopic understanding of NS made great progresses.
But we would like to know why NS is so heavy and large.

Microscopic study (nuclear physics exp) becomes more important than ever!

Two proposals to solve the “hyperon puzzle”

PR12-24-013

An isospin dependence study of the Lambda-N interaction through the high precision spectroscopy of Lambda hypernuclei with electron beam.

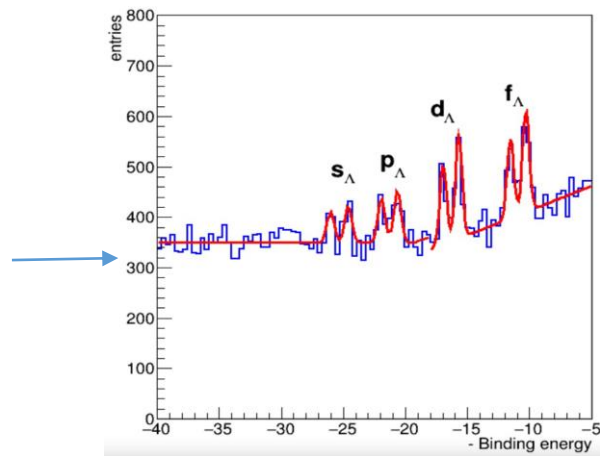
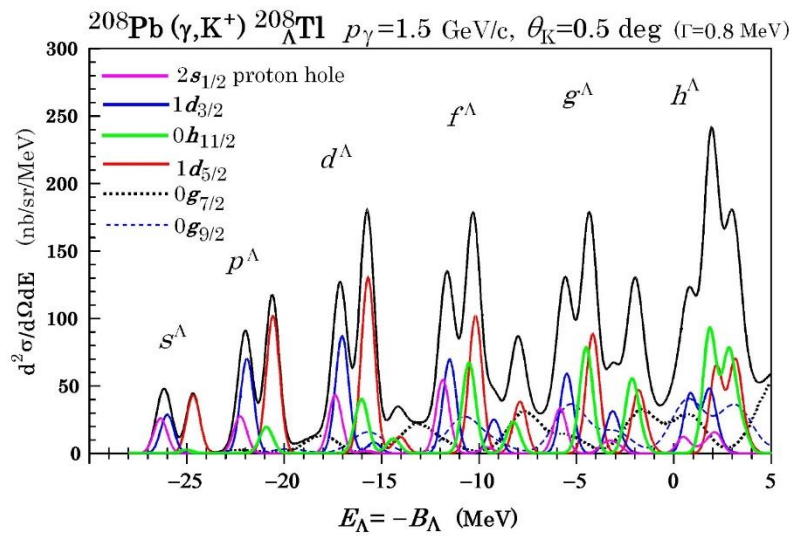
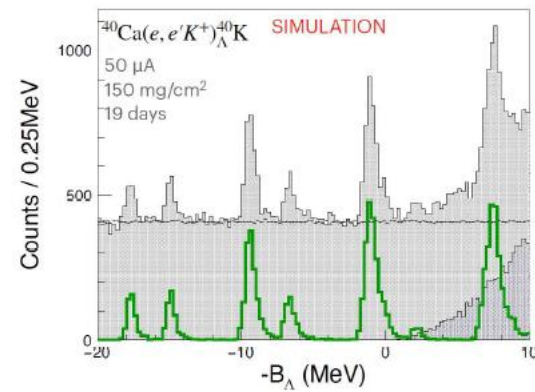
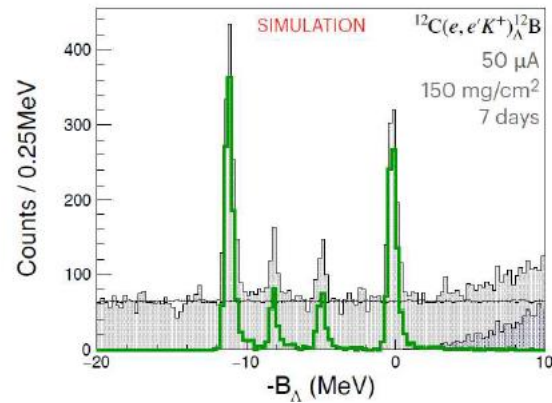
Neutron stars are 90% made up of neutrons. The effect of **asymmetry of the nuclear medium** on the hyperon chemical potential can be translated into **an isospin dependence of YNN interaction**. Very accurate measurements of asymmetric hypernuclei binding energies are hence necessary. According to Auxiliary-Field Diffusion Monte Carlo (AFMC) calculations, **if the three-body Λ NN repulsive force has isospin dependence** it would result in a shift in the energy dependence when the **neutron-rich ${}^{48}_{\Lambda}K$** target is used. On the other hand the effect of **isospin dependence is small for the target ${}^{40}_{\Lambda}K$** with equal numbers of protons and neutrons.

PR12-24-003

Studying Λ interactions in nuclear matter with the ${}^{208}Pb(e, e'K^+){}^{208}_{\Lambda}Tl$ reaction

The measured **charge density distribution of ${}^{208}Pb$** clearly shows that the **region of nearly constant density** accounts for a **very large fraction (~70 %) of the nuclear volume**, thus suggesting that its properties largely **reflect those of uniform nuclear matter in the neutron star**

The validity of this conjecture has been long established by a comparison between the results of **theoretical calculations and the data extracted from the ${}^{208}Pb(e, e'p){}^{207}Tl$ cross sections measured at NIKHEF in the 1990s**



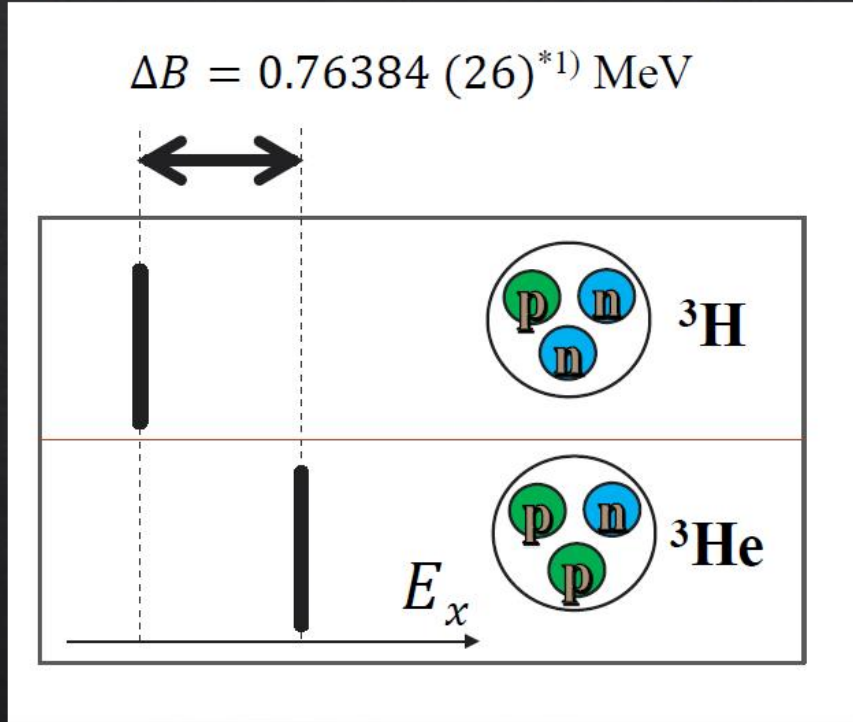
Bound state	Binding energy error (keV)
s_{Λ} (most bound)	172
s_{Λ} (less bound)	145
p_{Λ} (most bound)	81
p_{Λ} (less bound)	66
d_{Λ} (most bound)	58
d_{Λ} (less bound)	44
f_{Λ} (most bound)	61
f_{Λ} (less bound)	43

1000 simulated binding energy spectra, generated randomly with the expected background and with events generated randomly according to 8 gaussian distributions positioned at the locations and with the heights expected in the binding energy spectrum for the 8 most bounded states, were fitted

Charge symmetry breaking

Charge Symmetry Breaking (CSB), the mystery

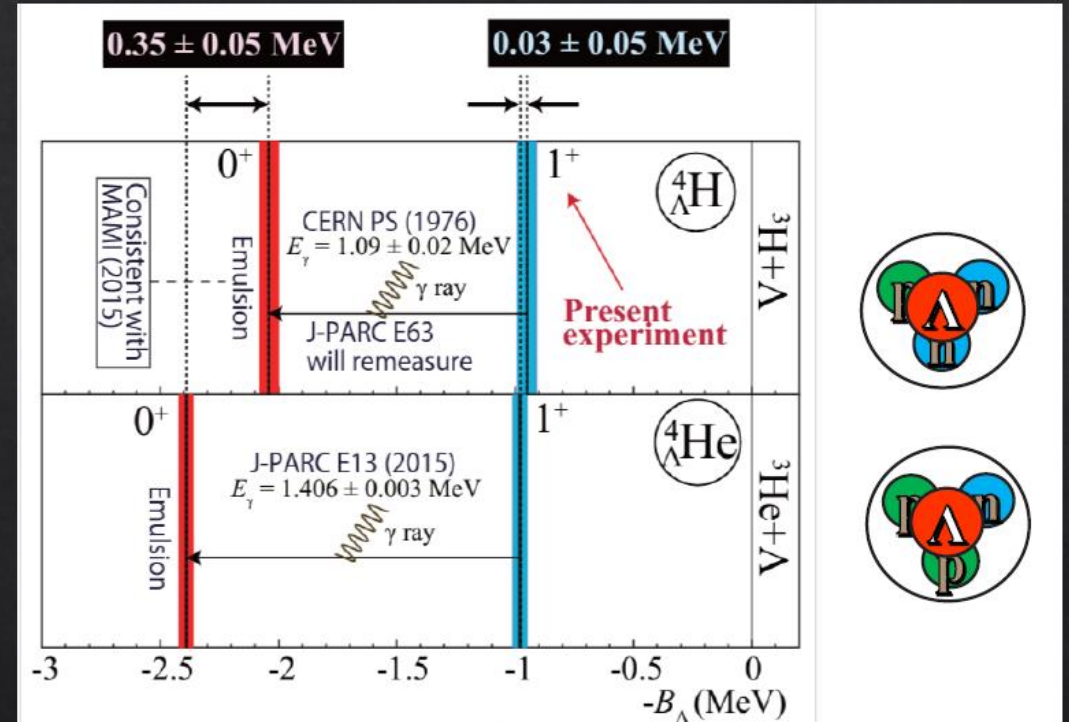
*1) J.H.E.Mattauch *et al.*, *Nucl. Pys.* 67, 1 (1965).



81 keV after Coulomb correction

[R.A.Brandenburg, S.A.Coon *et al.*, *NPA294*, 305 (1978)]

Figure from proposal of [JLab E12-19-002](#)



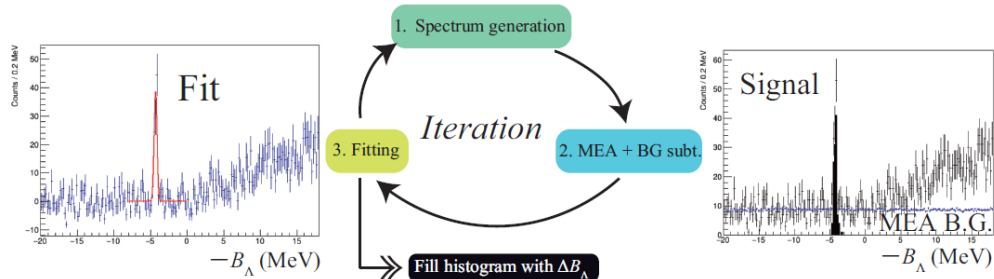
~400 KeV after Coulomb correction

➔ **5 times larger CSB than NN interaction!**

Proposal PR12-24-004


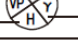
Study of Charge Symmetry Breaking in p-shell hypernuclei

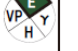









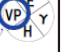
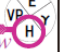



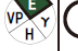








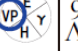

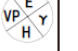





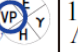

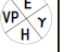





${}^6_{\Lambda}\text{He}$, ${}^9_{\Lambda}\text{Li}$, and ${}^{11}_{\Lambda}\text{Be}$ spectroscopy



Isomultiplet	${}^4_{\Lambda}\text{He}-{}^4_{\Lambda}\text{H}$	${}^7_{\Lambda}\text{Be}-{}^7_{\Lambda}\text{Li}^*$	${}^7_{\Lambda}\text{Li}^*-{}^7_{\Lambda}\text{He}$	${}^8_{\Lambda}\text{Be}-{}^8_{\Lambda}\text{Li}$	${}^9_{\Lambda}\text{B}-{}^9_{\Lambda}\text{Li}$	${}^{10}_{\Lambda}\text{B}-{}^{10}_{\Lambda}\text{Be}^*$
Shell model (Gal <i>et al.</i>) [41]	+226	-17	-28	+49	-54	-136
Cluster model (Hiyama <i>et al.</i>) [39, 40]		+150	+130			+20
No-core shell model (Le <i>et al.</i>) [43]	+238	-35	-16	+143		
Experiment	$+233 \pm 92$	-100 ± 90	-20 ± 230	$+40 \pm 60$	-210 ± 220	-220 ± 250

Existing data accuracy is sufficient for CSB study.

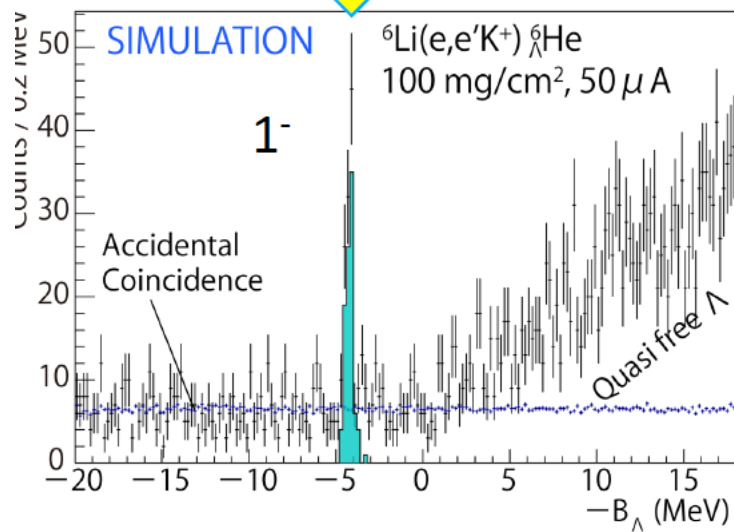
Electron-beam experiment at JLab  Emulsion experiment
Hadron-beam experiment at J-PARC  γ -ray experiment

Hypernucleus		T<0	T=0	T>0	CSB study		
					Now	New JLab	J-PARC
s-shell	$d N \Lambda$ (0^+)	${}^4_{\Lambda}\text{H}$ 		${}^4_{\Lambda}\text{He}$ 			
	$d N \Lambda$ (1^+)	${}^4_{\Lambda}\text{H}$  <i>new</i>		${}^4_{\Lambda}\text{He}$ 			
p-shell	$\alpha N \Lambda$	${}^6_{\Lambda}\text{He}$  <i>new</i>		${}^6_{\Lambda}\text{Li}$  <i>new</i>			
	$\alpha N N \Lambda$	${}^7_{\Lambda}\text{He}$ 	${}^7_{\Lambda}\text{Li}^*$ 	${}^7_{\Lambda}\text{Be}$ 			
	$\alpha d N \Lambda$	${}^8_{\Lambda}\text{Li}$ 		${}^8_{\Lambda}\text{Be}$ 			
	$\alpha d N N \Lambda$	${}^9_{\Lambda}\text{Li}$  <i>new</i>	${}^9_{\Lambda}\text{Be}$ 	${}^9_{\Lambda}\text{B}$ 			
	$\alpha \alpha N \Lambda$	${}^{10}_{\Lambda}\text{Be}$ 		${}^{10}_{\Lambda}\text{B}$  <i>new</i>			
	$\alpha \alpha N N \Lambda$	${}^{11}_{\Lambda}\text{Be}$  <i>new</i>	${}^{11}_{\Lambda}\text{B}$  <i>new</i>	${}^{11}_{\Lambda}\text{C}$ 			
	$\alpha \alpha d N \Lambda$	${}^{12}_{\Lambda}\text{B}$ 		${}^{12}_{\Lambda}\text{C}$  <i>new</i>			

Expected Spectra

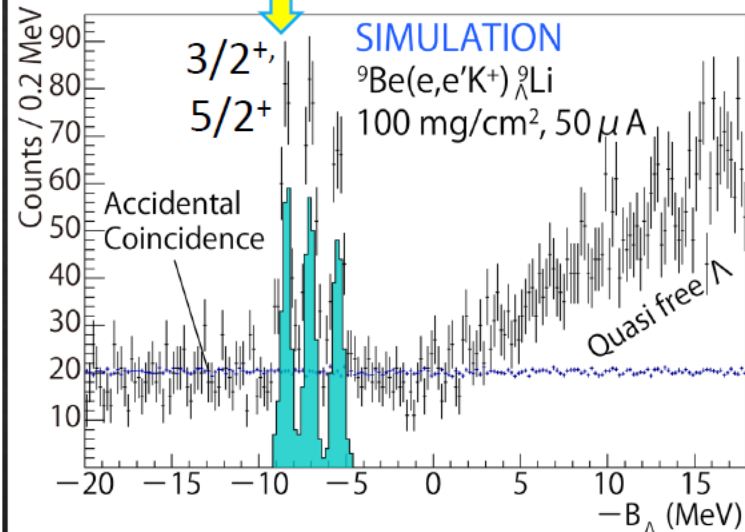
for CSB study

120 hours



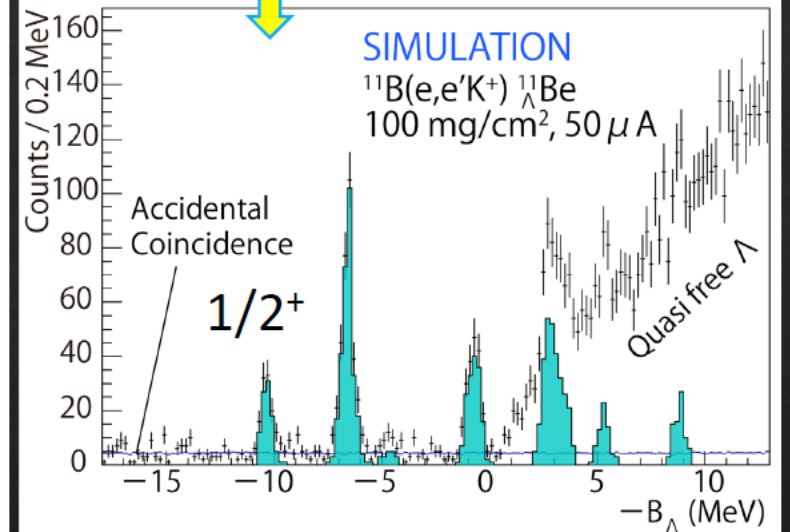
for CSB study

384 hours



for CSB study

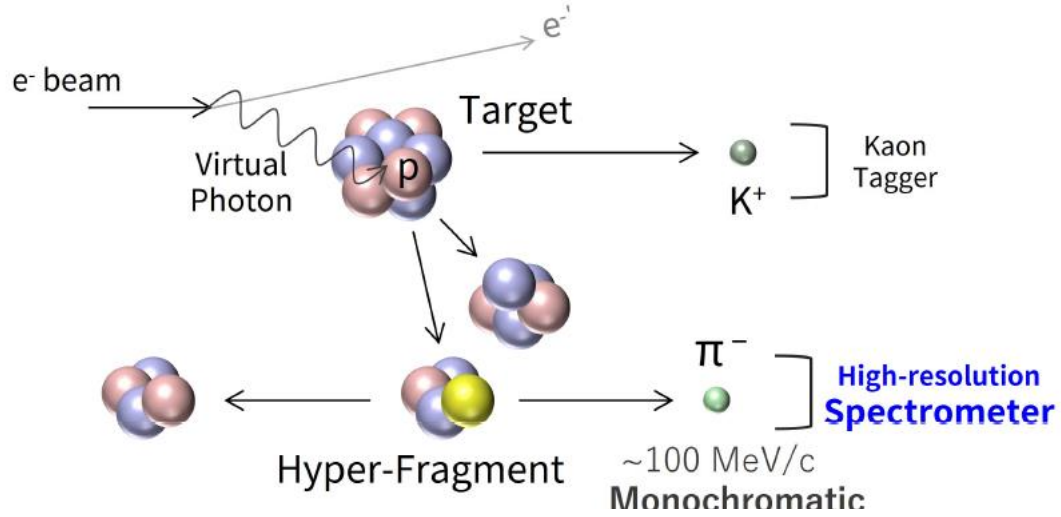
72 hours



Total accuracy:

$$|\Delta B_{\Lambda}^{\text{total}}| = \sqrt{(\Delta B_{\Lambda}^{\text{stat.}})^2 + (\Delta B_{\Lambda}^{\text{sys.}})^2} \leq 70 \text{ keV}$$

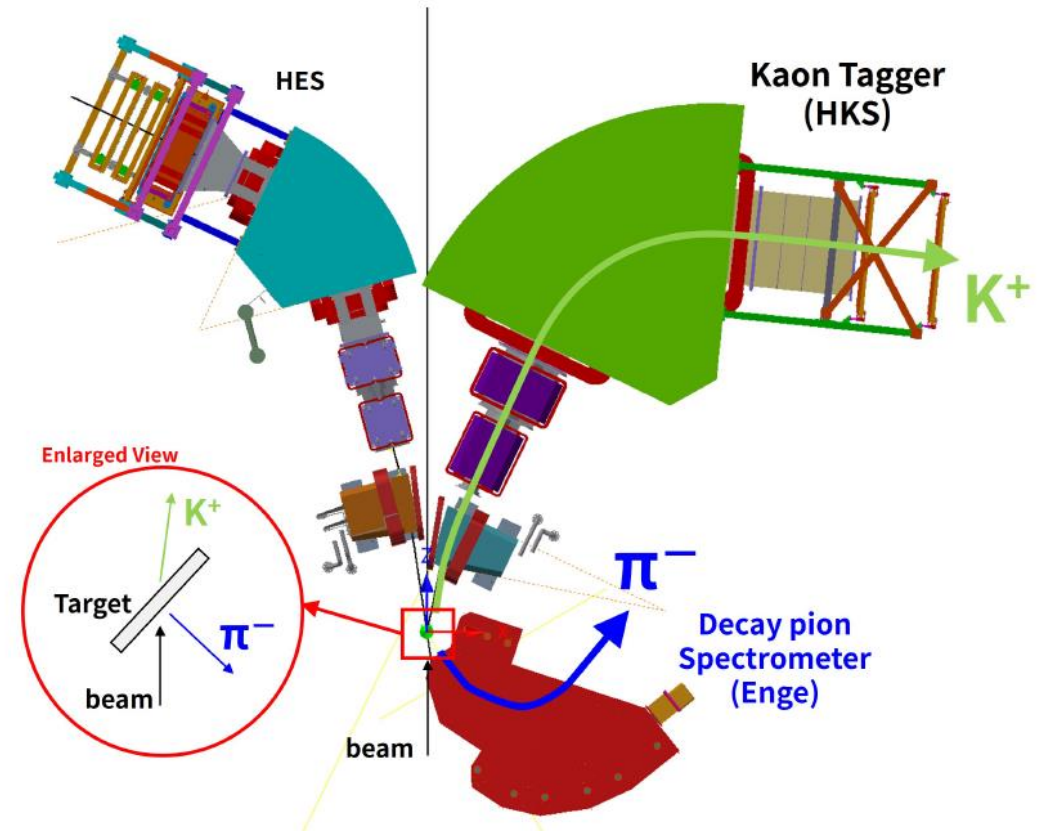
Run Group Addition E12-20-013A/E12-15-008A

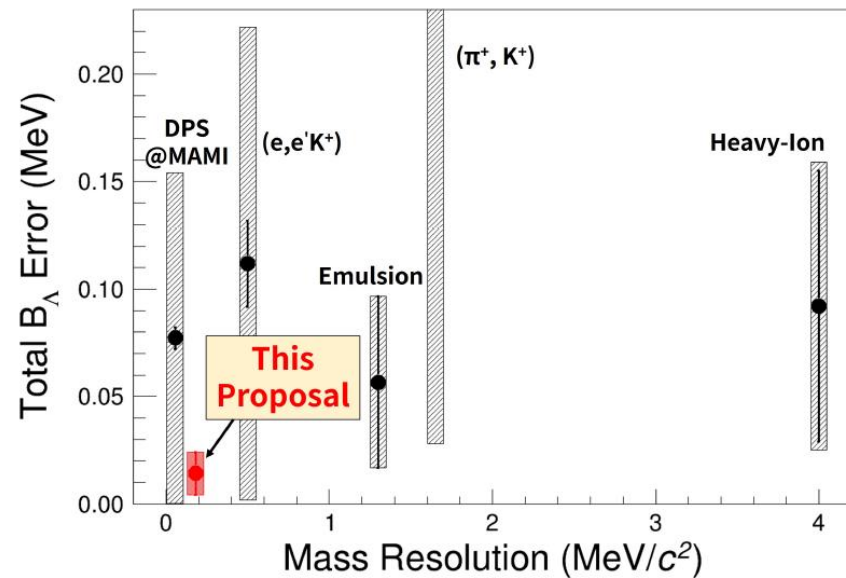


$$B_\Lambda = M_{\text{core}} + M_\Lambda - M_{\text{HYP}}, \quad M_{\text{HYP}} = \sqrt{M_{\text{nucl}}^2 + p_{\pi^-}^2} + \sqrt{M_{\pi^-}^2 + p_{\pi^-}^2}.$$

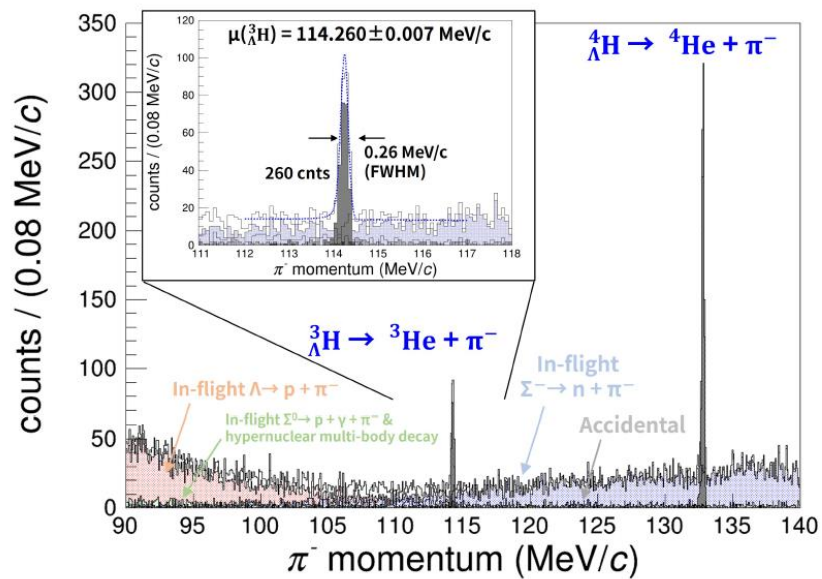
Hypernuclei	Decay mode	p_{π^-} (MeV/c)
${}^3_\Lambda\text{H}$	${}^3\text{He} + \pi^-$	114.4
${}^4_\Lambda\text{H}$	${}^4\text{He} + \pi^-$	133.0
${}^6_\Lambda\text{H}$	${}^6\text{He} + \pi^-$	135.3
${}^7_\Lambda\text{He}$	${}^7\text{Li} + \pi^-$	115.1
${}^7_\Lambda\text{Li}$	${}^7\text{Be} + \pi^-$	108.1
${}^8_\Lambda\text{He}$	${}^8\text{Li} + \pi^-$	116.5
${}^8_\Lambda\text{Li}$	${}^8\text{Be} + \pi^-$	124.2
${}^8_\Lambda\text{Be}$	${}^8\text{B} + \pi^-$	97.2
${}^9_\Lambda\text{Li}$	${}^9\text{Be} + \pi^-$	121.3
${}^9_\Lambda\text{B}$	${}^9\text{C} + \pi^-$	96.8
${}^{10}_\Lambda\text{B}$	${}^{10}\text{C} + \pi^-$	100.5
${}^{11}_\Lambda\text{B}$	${}^{11}\text{C} + \pi^-$	86.5
${}^{12}_\Lambda\text{B}$	${}^{12}\text{C} + \pi^-$	115.9

A list of expected pion momenta

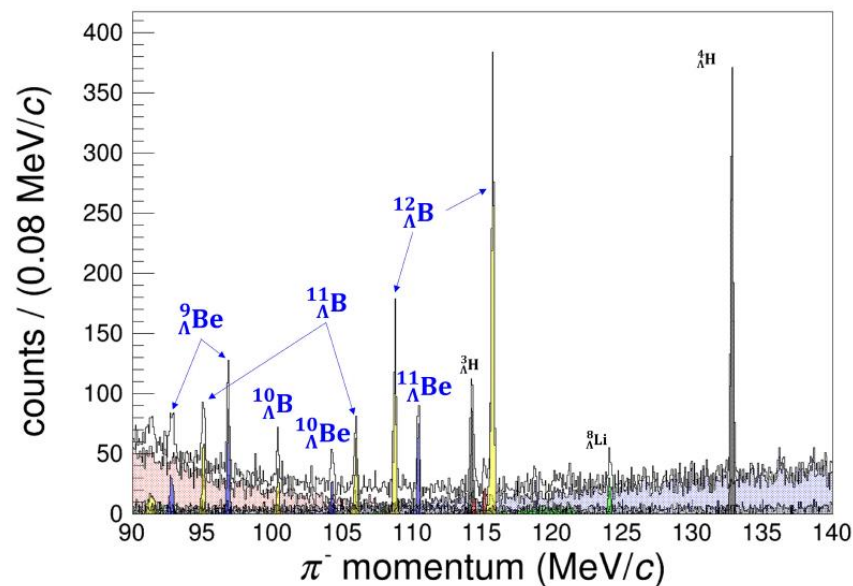




Pion spectra



Li target



Graphite target

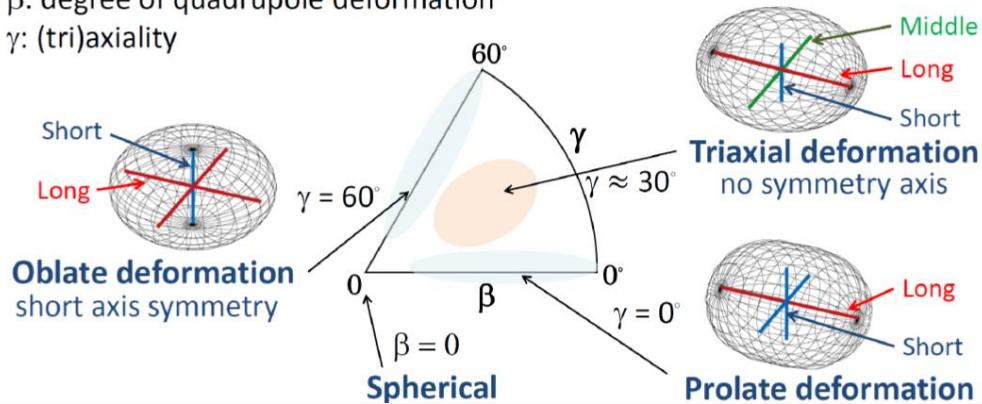
Study on the nucleus deformations

Study of triaxially deformed nucleus using a Lambda particle as a probe

Parameters to describe deformation

Nuclear quadrupole deformation (β, γ)

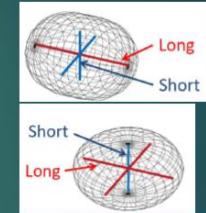
- β : degree of quadrupole deformation
- γ : (tri)axiality



^{26}Mg is interesting candidate for triaxially deformed nucleus

Proton $Z=12$ Prolate

Neutron $N=14$ Oblate

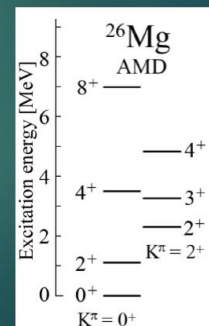
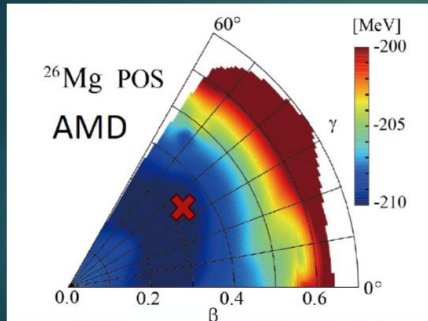


Co-existence of different deformations

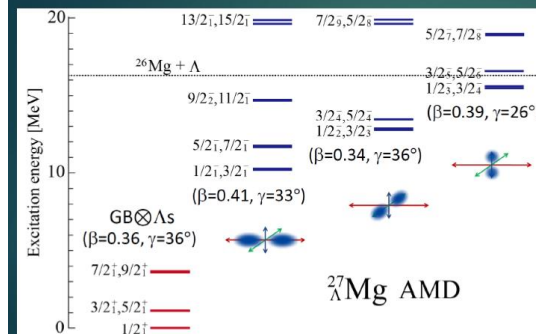
- Terasaki et al. NPA621(1997)
- Rodriguez-Guzman et al. NPA709 (2002)
- Peru et al PRC77 (2008)
- Hinohara, Kanada-En'yo PRC83 (2011)

Recent theoretical calculation

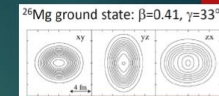
(Hyper) Anti-symmetrized Molecular Dynamics
M. Isaka et al. PRC 83 (2011) 044323.
PRC 83 (2011) 054304.



Adding a Λ particle

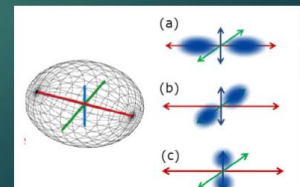


M. Isaka, Hypernuclear Physics Workshop 2023 at JLab



ΛN interaction is attractive
WF of Λ in p-orbit is straight
Overlap between Λ and ^{26}Mg core depends on axis direction

$^{26}\text{Mg} \otimes \Lambda(p)$ splits in 3 states



Schedule

- Experimental Readiness Review (EER)
scheduled on November -December 2024
- Apparatus installation: 2026
- Experiment run 2027

Rivelatori microstrip di silicio

Sta per finire la messa a punto e caratterizzazione di due piani (X,Y) di rivelatori microstrip di silicio. Ciascun piano sarà formato da due rivelatori microstrip di silicio di $10 \times 10 \text{ cm}^2$ di superficie, cosicché la superficie totale di ciascuno dei due piani sarà di $20 \times 10 \text{ cm}^2$. Pitch dei rivelatori: $50 \text{ }\mu\text{m}$

Un possibile impiego dei rivelatori microstrip di silicio:

Come sieve slit attive negli esperimenti di spettroscopia ipenucleare

Questi esperimenti erano inizialmente programmati per aver luogo in Hall A, ed erano stati approvati dal PAC di JLab.

Tuttavia, la necessità di runnare in Hall A il prima possibile l'esperimento MOLLER ha spinto il management di Jlab a chiedere che questi esperimenti avessero luogo in Hall C. Questo ha comportato alcune difficoltà nell'adattare agli spettrometri della Hall C i due setti magnetici (Particle Charge Separator /PCS), appositamente disegnati per essere posti davanti agli spettrometri di Hall A per permettere ad essi di rivelare particelle diffuse a piccolo angolo.

In particolare, se si tentasse di riprodurre lo stesso setup sperimentale previsto in Hall A, la sieve slit box montata sull'entrata della camera a vuoto del PCS posto davanti allo spettrometro impiegato per la rivelazione dei Kaoni (HKS) interferirebbe con il beam pipe. Questo costringe a uno spostamento indietro dell'intero sistema PCS + HKS di circa 17.8 cm con perdita dell'angolo solido dello spettrometro. Tutto questo potrebbe essere evitato utilizzando, al posto delle sieve slit «classiche», i piani di microstrip di silicio per determinare (tra l'altro con estrema precisione) gli angoli di diffusione delle particelle nei run di calibrazione effettuati per determinare i data base ottici degli spettrometri.